SERBIAN JOURNAL OF ELECTRICAL ENGINEERING
Vol. 12, No. 1, February 2015, 81-98

UDC: 007.52:519.87 **DOI: 10.2298/SJEE1501081P**

Compliant Behaviour of Redundant Robot Arm - Experiments with Null-Space

Petar B. Petrović[1], Nikola Lukić[1], Ivan Danilov[1]

Abstract: This paper presents theoretical and experimental aspects of Jacobian nullspace use in kinematically redundant robots for achieving kinetostatically consistent control of their compliant behavior. When the stiffness of the robot endpoint is dominantly influenced by the compliance of the robot joints, generalized stiffness matrix can be mapped into joint space using appropriate congruent transformation. Actuation stiffness matrix achieved by this transformation is generally nondiagonal. Off-diagonal elements of the actuation matrix can be generated by redundant actuation only (polyarticular actuators), but such kind of actuation is very difficult to realize practically in technical systems. The approach of solving this problem which is proposed in this paper is based on the use of kinematic redundancy and nullspace of the Jacobian matrix. Evaluation of the developed analytical model was done numerically by a minimal redundant robot with one redundant d.o.f. and experimentally by a 7 d.o.f. Yaskawa SIA 10F robot arm.

Keywords: Kinematic redundancy, Compliance control, Null space stiffness.

1 Introduction

Regardless of its mechanical and kinematical composition, any robot is an elastomechanical structure which deforms while interacting with the environment. Contrary to other elastomechanical mechanisms, compliant behavior of the robot mechanism can be controlled actively.

Compliance is essential for robot tasks which include constrained motion of the robot endpoint, or other movable parts of robot mechanism. Since small errors in model acquisition and estimation can be compensated, compliance in motion control enables robots to be effectively used in tasks where such errors are present. Compliance is important for explorative activities in insufficiently structured environment and when the environment changes in time. This also includes the environment populated by humans, in which physical proximity and physical interaction with humans is expected or planned, as it happens in collaborative tasks with human workers on manufacturing lines.

[1]Mechanical Engineering Faculty, University of Belgrade, Kraljice Marije 16, 11000 Belgrade, Serbia; E-mails: pbpetrovic@mas.bg.ac.rs; nlukic@mas.bg.ac.rs; idanilov@mas.bg.ac.rs

Compliance in robot mechanism is assumed to be distributed at joints and links, i.e., the mechanical structure which connects neighboring joints. In most cases robot links are sufficiently stiff and their contribution to the overall compliance of the robot can be neglected. It is worth to mention that this is exactly the case in biomechanical systems, like human limbs, for instance.

For modeling purposes in kinetostatic domain, robot can be considered as a kinematic mechanism with rigid links and compliant, or more precise, soft joints. Therefore, the study of flexibility concentrated in joints and nature of its contribution to the compliance of robot mechanism is of highest practical importance. Robot compliant behavior considered in this paper is limited to the robots with flexible joints only.

Probably the earliest investigation of Jacobian nullspace and its use for control of secondary tasks execution is related to the research work presented in [1]. Later on, this approach is further developed and formulated as the 'extended Jacobian technique' [2]. The term 'extended' is related to the generalization of the inverse kinematic problem by superposition of the particular solution for the linear mapping defined by Jacobian matrix and associated homogeneous part of this mapping which always exists in underdefined linear (and linearized) systems like this one which is present in kinematically redundant mechanisms.

Although the nullspace of redundant robots is deeply studied in kinematic domain, this is not the case with their compliant behavior. Although the compliance behavior is not explicitly considered, results which are related to the Jacobian nullspace and the external force projected into the robot jointspace is presented in [3]. Later on, this is addressed explicitly to the robot stiffness control in [4]. Probably the most comprehensive study of compliance in redundant robot mechanisms and its active control is given in [5]. Despite the efforts done in this domain (especially in recent time when applications with physical human-robot interaction are exponentially growing [6]), formally complete and practically applicable framework of stiffness control based on nullspace of kinematically redundant robots still does not exist.

In our research we have found that the kinematic redundancy can be very efficiently exploited to induce the desired robot generalized stiffness only by robot internal motion within the associated nullspace. In this context, this paper presents very general theoretical and experimental aspects of the use of Jacobian nullspace in kinematically redundant robots for achieving kinetostatically consistent control of their compliant behavior in the task space. The paper is organized as follows: the concept of generalized stiffness and jointspace stiffness is given in Section 2; Generalized virtual displacement of the robot endpoint and complementary nullspace projector are formulated in Section 3; Proposed cost function for canonization of the jointspace stiffness matrix is presented in Section 4; Numerical example based on a minimal

redundant robot and preliminary experimental results achieved with the 7 d.o.f. Yaskawa SIA10F robot arm is given in Section 5.

2 Generalized Stiffness

The concept of generalized stiffness is derived from the generalization of the robot arm elastomechanical behavior as shown in Fig. 1. In the case of the robot arm with flexible joints and rigid links, the endpoint, or equivalently, the tool center point (TCP) generalized stiffness, is defined by following equation:

$$F_{TCP} = K_x(x - x_0) = K_x \delta x_{TCP}, \tag{1}$$

where $F_{TCP} \in R^m$ is the external force which excites the robot mechanism at the robot TCP (robot-environment contact force), $K_x = K_{TCP} \in R^{m \times m}$ is the TCP generalized stiffness matrix, $x \in R^m$ is the vector of the robot current TCP position, and $\delta x \in R^m$ is the TCP displacement vector, induced by F_{TCP}.

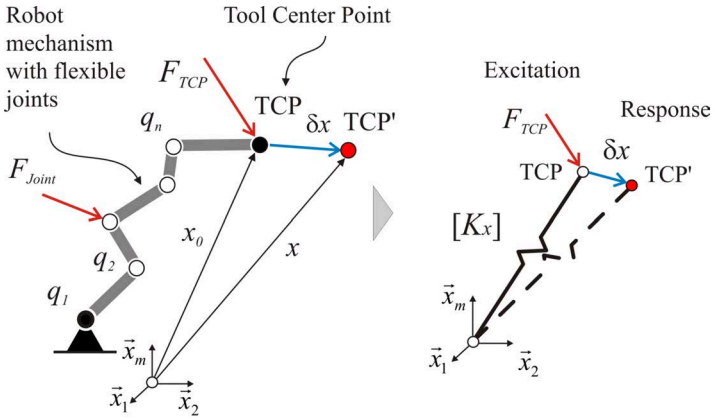

Fig. 1 – *Reduction of the serial link robot arm to a generalized spring.*

Mapping of the generalized stiffness matrix (1) into the robot jointspace can be analytically achieved by applying the energy conservation principle [4]:

$$\delta W_\tau \equiv \delta W_F + \delta W_g + \delta W_\mu, \tag{2}$$

where δW_τ is the virtual work associated with the joint torques, δW_F is the work associated with the external force, δW_g is the work associated with the gravitational forces, and δW_μ is the virtual work associated with the frictional forces. If gravitational and frictional terms are neglected, the equation (2) becomes:

$$\delta W_\tau \approx \delta W_F, \tag{3}$$

that immediately leads to:

$$\tau^T \delta q = F_{TCP}{}^T \delta x_{TCP}\,, \tag{4}$$

where τ is the joint torque vector and δq is the corresponding joint displacement vector. Substituting:

$$\delta x_{TCP} = J(q)\delta q\,, \tag{5}$$

into (4) leads to the very important equation which defines mapping of external force from the robot task space to the corresponding joint torques vector, and vice versa:

$$\tau = J^T(q) F_{TCP}\,. \tag{6}$$

This equation can be understood as a matrix relation which defines the static balance conditions between the external force applied to the robot TCP and corresponding torques which are generated by the joint actuators of the robot mechanism. The $J(q)$ stands for Jacobian matrix, which is composed of gradients that linearly map displacements of the robot TCP into the robot joint displacements.

External force in (6) can be substituted by the generalized stiffness matrix using (1), which leads to the relation:

$$\tau = J^T(q) K_x J(q) \delta q\,. \tag{7}$$

Congruent transformation of the robot TCP stiffness matrix K_x is in fact, required linear mapping of the robot mechanism generalized stiffness into the jointspace stiffness matrix K_q [7]:

$$K_x \rightarrow K_q(q, K_x) = J^T(q) K_x J(q), \;\; K_q \in R^{n \times n}\,. \tag{8}$$

Elements of the jointspace stiffness matrix (8) are nonlinear functions of the generalized stiffness matrix and the robot joint coordinates. It means that the jointspace stiffness matrix is sensitive to the robot configuration, i.e., robot posture. Also, the jointspace stiffness matrix defined by (8) is in general nondiagonal matrix. That means that off-diagonal elements are not equal to zero:

$$k_{q\_ij} = f_{q\_ij}(q, K_{xd}), \qquad k_{q\_ij} \neq 0, \quad \forall i \neq j \tag{9}$$

As a consequence of previously stated, a nonredundant robot which is capable to generate an arbitrary generalized stiffness matrix, needs to be driven with the redundant actuators, i.e., polyarticular actuators. For example, in 2 d.o.f. SCARA robot, an additional third actuator needs to be provided, in parallel with already existing monoarticular actuators (Fig. 2). This actuator simultaneously affects both joints at the same time (biarticular actuator). In this simple example the difference between the jointspace stiffness matrices generated by the kinematically nonredundant robot which is driven by the monoarticular actuators only:

$$K_q = \begin{bmatrix} k_{q1} & 0 \\ 0 & k_{q2} \end{bmatrix}, \tag{10}$$

and the same robot, but with additional biarticular actuator:

$$K_q = \begin{bmatrix} k_{q1} + k_X & k_X \\ k_X & k_{q2} + k_X \end{bmatrix} \tag{11}$$

can be easily recognized. Apparently, the influence of introduced biarticular actuator is very strong, since it is present in all entries of the jointspace stiffness matrix and, the most important, the off-diagonal elements are no longer equal to zero. It is clear that actuation redundancy can provide the robot control system with ability to generate an arbitrary desired generalized stiffness matrix of its TCP. But, there is one very important problem: the technical complexity of redundant actuation, especially the complexity of the actuator which is capable to generate the biarticular actuation, is very high. Up to now, no robot which is commercially available and driven by redundant actuation concept exists out of laboratories.

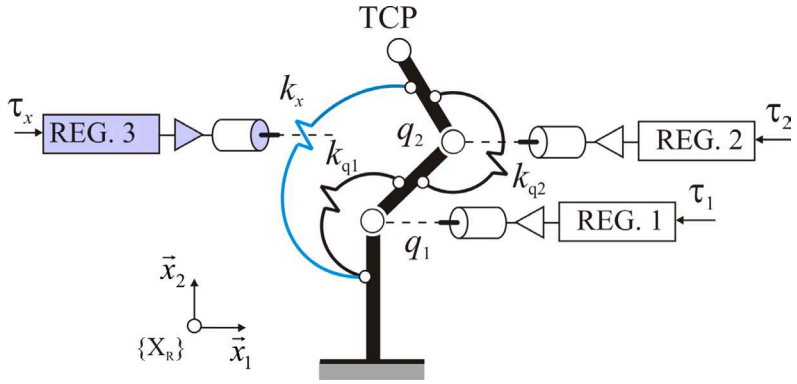

Fig. 2 – *Planar 2 d.o.f. robot arm actuated by biarticular actuator.*

It is worth to mention that the actuation redundancy of this type is very frequent in biomechanical systems, including human arms [8, 9]. Biarticular muscles of a human upper arm are shown in Fig. 3. Two dominant muscles, biceps and triceps, simultaneously actuate shoulder and elbow joints.

In order to solve this problem an analytical framework which is based on kinematic redundancy instead of actuation redundancy is developed. Kinematic redundancy is technically much simpler to realize than actuation redundancy, but its practical application is often faced with extremely high computational burden.

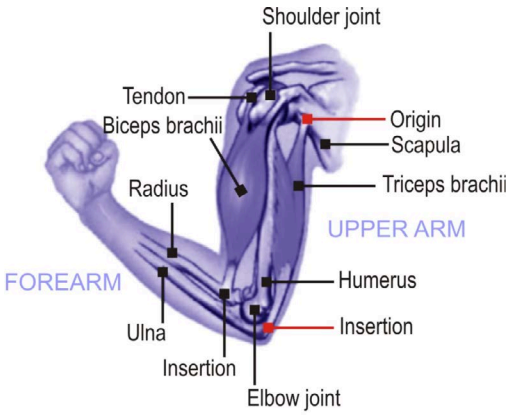

Fig. 3 – *Biarticular muscles in human upper arm that redundantly drive shoulder and elbow joints.*

3 Generalized virtual displacement

Starting point of exploiting the kinematic redundancy as a general framework for finding technical solutions which satisfy (8) is based on the following hypothesis: Within the nullspace of the kinematically redundant robot with r redundant degrees of freedom, exists at least one configuration subspace with a nonempty set of configurations (robot postures) which simultaneously satisfies: 1) the nominal position x_0 of the robot TCP point – the primary task, 2) the desired generalized stiffness K_{xd} of the robot TCP - the secondary task (the additional tasks must be represented as a function of robot joint coordinates, [1, 10]), and 3) the canonical form of the corresponding actuation stiffness matrix K_q that is consistent with robot desired TCP stiffness matrix K_{xd}. This hypothesis is based on the assumption that the increased mobility / dexterity of the kinematically redundant robot mechanism which is actuated by a set of variable stiffness monoarticular actuators can effectively generate arbitrary desired generalized stiffness of the robot TCP on a technically acceptable way. Internal structure of the TCP stiffness matrix is discussed in [11, 12].

The nullspace of Jacobian matrix denoted by $\mathrm{N}(J(q))$, is defined as:

$$\mathrm{N}(J(q)) = \left\{ \delta q \in R^{m \times n} : \; J(q)\delta q = 0 \right\}. \tag{12}$$

Nullspace (12) is in fact a set of nontrivial solutions of the homogeneous system of linear equations associated to the Jacobian matrix:

$$J(q)\delta q = 0_n. \tag{13}$$

Contrary to the nonredundant robot mechanism, inverse kinematic of the kinematically redundant robot has a more general solution, which is composed

of two components: the nonhomogeneous member, i.e., particular solution δq_P of the nonhomogeneous linear system (5), and the homogeneous member, i.e., the solution δq_N which belong to the nullspace of Jacobian matrix, (13). This leads to the definition of the generalized virtual displacement which is analytically defined by the following relation:

$$\delta q = \delta q_P + \delta q_N = J^+(q)\delta x + P^c{}_{N(J)}(q)\delta q_0 , \tag{14}$$

where: $J^+(q)$ is the generalized inverse of the Jacobian matrix $J(q)$ which satisfies Moore-Penrose least norm condition [13], δq_0 is an arbitrary vector in the robot configuration space, and $P^c{}_{N(J)}$ is the complementary projector, i.e., an operator which projects the vector δq_0 to the nullspace of Moore-Penrose generalized inversion $J^+(q)$ of the Jacobian matrix. Equations (12) – (14) are graphically shown in Fig. 4.

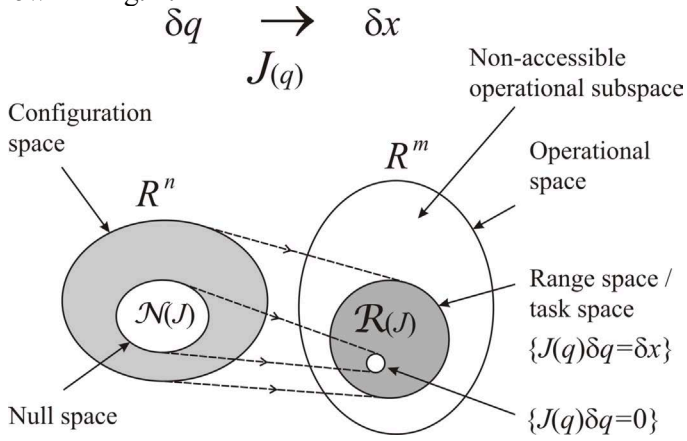

Fig. 4 – *Graphical presentation of the robot configuration and operational space, as well as the Jacobian rang space and nullspace.*

Homogeneous member in (14) is the formal vehicle which can be used for generation of internal motions in the robot mechanism, i.e., selfmotions which do not alter the robot TCP position. Since the jointspace stiffness matrix is dependant of the robot joint coordinates, (8), internal motions in the Jacobian nullspace will affect the jointspace stiffness matrix. In that sense, nullspace motion can be used to satisfy secondary task objective, [1, 2]. That is control of generalized stiffness of the robot TCP. Since the nullspace motions have no influence to the robot TCP motion, equation (14) allows that primary task will be accomplished independently.

Equation (14) can be interpreted as an inference machine that provides formally consequent superpostion of the primary task: position and motion

control of the robot arm and any other task of secondary priority – nonconflincting inclusion of secondary task into primary control task.

In accordance to [2] and [13], the complementary projector in (14) is defined by the following relation:

$$P^{c}{}_{N(J)}(q) = I - P_{N(J)}(q) = I - J^{+}(q)J(q), \tag{15}$$

while the Moore-Penrose generalized inverse is given by the following relation, [13]:

$$J^{+}(q) = J^{T}(q)\left(J(q)J^{T}(q)\right)^{-1} \in R^{n\times m}, \tag{16}$$

Relations (14) to (16) are essential for the approach which is proposed in this paper.

4 The Cost Function

Since in kinematically redundant robot mechanisms TCP force vector can be induced by infinite number of robot configurations, an arbitrary vector δq_0 in (14) which is projected into the robot nullspace by the complementary projector (15) can be used to control of the robot jointspace stiffness. To do that an appropriate cost function has to be defined. Probably the most relevant research results are presented in [11] where three cost functions are proposed for the general framework for robot TCP stiffness control.

The main requirement for the cost function is to minimize the influence the off-diagonal elements of the jointspace stiffness matrix (8) to the induced generalized stiffness matrix of the robot TCP:

$$K_x(q, K_q, t) = J^{-T}(q)K_q J(q)^{-1}, \;\; K_x \in R^{m\times m}, \tag{17}$$

which further on leads to the following definition of the nullspace vector optimization criterion:

$$\delta q_0 = \left\{ \delta q_0 \in R^n \,\middle|\, \delta q_0 = \min(\Delta K_q), \quad \Delta K_q = K_{qd} - K_q \right\}. \tag{18}$$

According to the relation (14) in this paper is proposed the cost function to be the Euclidean norm of the off-diagonal elements of the jointspace stiffness matrix (8):

$$u(q) = \left\| k_{q\_ij}(q) \right\|_{[\frac{n}{2}(n-1)]}, \quad \forall i \neq j. \tag{19}$$

Relation (19) generates the scalar potential field over the robot hyperdimensional configuration space. Since the potential field (19) is a nonlinear, continuous, and therefore differentiable function, the gradient optimization method can be effectively applied for finding of optimal nullspace

joint vector which locally minimizes influence of the cross-joint members of the robot jointspace stiffness matrix. This leads to the following relation:

$$\delta q_0 = -\alpha \nabla u(q) = -\alpha \frac{\partial}{\partial q} u(q), \quad \alpha > 0 . \tag{20}$$

Gradient optimization method is known to be algorithmically stable and always converges to the nearest local minimum. This algorithm is discrete in its essence, and therefore very suitable for application on digital control systems, using the following integration scheme:

$$q(t_{k+1}) = q(t_k) + \delta q(t_k) , \tag{21}$$

where $\delta q(t_k)$ is defined by (14).

In order to control the intensity of the δq_0 vector we multiply it with the scaling factor α. This scaling factor is very general, intuitive solution, which must be somehow related to additional constraints that can enable dynamically consistent nullspace displacements in (14). One of the possible intuitive solutions is given in [14].

In any single integration step of (21), the virtual displacement vector δq_0 is proportional to the negative gradient of the potential field (19). Therefore, it is not consistent with the nullspace kinematics of the robot arm mechanism. The scalar operator, $\alpha > 0$, is used to scale the magnitude of the δq_0. In that context, following relation is adopted:

$$\alpha(t_k) = \beta \frac{\left\| \delta q_P(t_k) \right\|}{\left\| \delta q_N(t_k) \right\|}, \quad \beta > 0 , \tag{22}$$

where β is the global multiplier, which is time independent and defined by the supervisor, or by the higher levels of the robot control system. The denominator of the fraction member in (22) is the magnitude of the displacement vector δq_N i.e., the cost function gradient projected onto the nullspace of the Jacobian pseudoinverse (16) using the complementary projector (14), and its role is to normalize the nullspace displacement vector δq_N. The numerator is the magnitude of the δq_P, which is the minimum norm displacement vector generated by the Moore-Penrose pseudoinverse. Note that the vector δq_P is calculated even when the primary task is completed, i.e., for the corresponding nullspace motions which are governed by the homogeneous solution δq_N of the (13). As a consequence, the α operator (22) is intrinsically adaptive and kinematically consistent.

5 Numerical Examples and Experiments

For evaluation purposes, kinematically redundant planar robot arm with 2d.o.f. is used with onedimensional task space. This robot has one redundant d.o.f. ($m = 1 \mid n = 2$ redundant anthropomorphic mechanism) / MRR-R1. The geometrical and kinematical variables of MRR-R1 are given in the Fig. 5. The analytical model of MRR-R1 is as follows. Direct kinematics of the MMR-R1 robot is:

$$\begin{aligned} x_1 &= f(q) = l_1 c_1 + l_2 c_{12} \\ c_1 &= \cos(q_1);\ c_{12} = \cos(q_1 + q_2) \end{aligned} \tag{23}$$

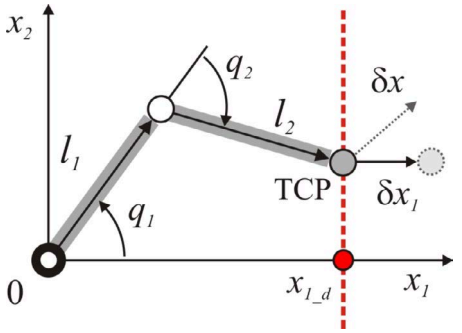

Fig. 5 – *Model of the minimal redundant robot with one redundant degree of freedom/MRR-R1.*

Jacobian matrix of the MRR-R1 is given by:

$$\begin{aligned} J(q) &= \begin{bmatrix} J_{1,1}(q) & J_{1,2}(q) \end{bmatrix} = \begin{bmatrix} -(l_1 s_1 + l_2 s_{12}) & -l_2 s_{12} \end{bmatrix} \\ s_1 &= \sin(q_1);\ s_{12} = \sin(q_1 + q_2) \end{aligned} \tag{24}$$

which leads to:

$$\delta x_1 = \begin{bmatrix} -(l_1 s_1 + l_2 s_{12}) & -l_2 s_{12} \end{bmatrix} \begin{bmatrix} \delta q_1 \\ \delta q_2 \end{bmatrix}. \tag{25}$$

Moore-Penrose pseudoinversion of Jacobian matrix (24) is:

$$J(q)^+ = \begin{bmatrix} J^+_{1,1}(q) \\ J^+_{2,1}(q) \end{bmatrix} = \begin{bmatrix} \dfrac{J_{1,1}(q)}{J_{1,1}(q)^2 + J_{1,2}(q)^2} \\ \dfrac{J_{1,2}(q)}{J_{1,1}(q)^2 + J_{1,2}(q)^2} \end{bmatrix}, \tag{26}$$

from which inverse kinematic model can be formulated as:

$$\delta q = J(q)^{+}\delta x,$$
$$\begin{bmatrix}\delta q_1\\ \delta q_2\end{bmatrix} = -\frac{1}{\left(l_1 s_1 + l_2 s_{12}\right)^2 + \left(l_2 s_{12}\right)^2}\begin{bmatrix} l_1 s_1 + l_2 s_{12}\\ l_2 s_{12}\end{bmatrix}\delta x_1. \tag{27}$$

Then the range space of the Jacobian matrix is:

$$\begin{bmatrix}\delta q_1\\ \delta q_2\end{bmatrix} = \begin{bmatrix} J^{+}_{1,1}(q)\\ J^{+}_{2,1}(q)\end{bmatrix}\delta x_1,$$
$$\delta q_1 = \frac{J^{+}_{1,1}(q)}{J^{+}_{2,1}(q)}\delta q_2 = \frac{l_1 s_1 + l_2 s_{12}}{l_2 s_{12}}\delta q_2. \tag{28}$$

Then, by transforming of the Jacobian matrix to the equivalent reduced row echelon form:

$$\begin{bmatrix}\left(l_1 s_1 + l_2 s_{12}\right) & l_2 s_{12}\end{bmatrix}\begin{bmatrix}\delta q_1\\ \delta q_2\end{bmatrix} = 0,$$
$$N(J(q)) = rref(J(q)) = \begin{bmatrix}1 & a_x\end{bmatrix}, \tag{29}$$
$$a_x = a_x(q) = \frac{J_{1,2}(q)}{J_{1,1}(q)} = \frac{l_2 s_{12}}{l_1 s_1 + l_2 s_{12}},$$

corresponding nullspace can be immediately analytically formulated:

$$\begin{bmatrix}1 & \frac{l_2 s_{12}}{l_1 s_1 + l_2 s_{12}}\end{bmatrix}\begin{bmatrix}\delta q_1\\ \delta q_2\end{bmatrix} = 0,$$
$$\delta q_1 = -\frac{J_{1,2}(q)}{J_{1,1}(q)}\delta q_2 = -\frac{l_2 s_{12}}{l_1 s_1 + l_2 s_{12}}\delta q_2. \tag{30}$$

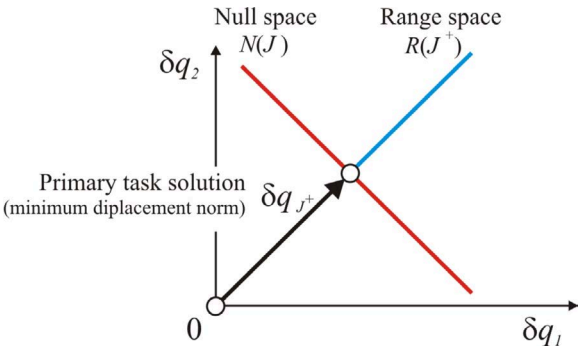

Fig. 6 – *Range space and nullspace of MRR-R1.*

It is clear from (28) and (30) that the range space and the nullspace of the Jacobian matrix (24) are straight line in the robot configuration space. This can be graphically depicted as it is given in the Fig. 6. It is worth to mention that the range space of the Jacobian matrix and its nullspace are orthogonal spaces (in this particular case, it is orthogonal lines). The particular solution of (14) which is related to the minimal norm pseudoinverse of Jacobian matrix is also shown in the Fig. 6.

Following the equation (14) the nullspace complementary projector can be directly calculated from the equation (15):

$$P^{c}_{N(J(q))} = \begin{bmatrix} \dfrac{J_{1,2}(q)}{J_{1,1}(q)^2 + J_{1,2}(q)^2} & -\dfrac{J_{1,1}(q)J_{1,2}(q)}{J_{1,1}(q)^2 + J_{1,2}(q)^2} \\ -\dfrac{J_{1,1}(q)J_{1,2}(q)}{J_{1,1}(q)^2 + J_{1,2}(q)^2} & \dfrac{J_{1,1}(q)}{J_{1,1}(q)^2 + J_{1,2}(q)^2} \end{bmatrix} = \\ = \begin{bmatrix} \dfrac{l_2 s_{12}}{\left(l_1 s_1 + l_2 s_{12}\right)^2 + \left(l_2 s_{12}\right)^2} & -\dfrac{\left(l_1 s_1 + l_2 s_{12}\right) l_2 s_{12}}{\left(l_1 s_1 + l_2 s_{12}\right)^2 + \left(l_2 s_{12}\right)^2} \\ -\dfrac{\left(l_1 s_1 + l_2 s_{12}\right) l_2 s_{12}}{\left(l_1 s_1 + l_2 s_{12}\right)^2 + \left(l_2 s_{12}\right)^2} & \dfrac{l_1 s_1 + l_2 s_{12}}{\left(l_1 s_1 + l_2 s_{12}\right)^2 + \left(l_2 s_{12}\right)^2} \end{bmatrix}, \tag{31}$$

which finally leads to the components of the nullspace vector which is governing the execution of the secondary control task, i.e., shaping of the generalized stiffness matrix of the robot TCP:

$$\delta q_{0N} = \left[1 - J^{+}(q)J(q)\right] \delta q_0 = \left[\delta q_{0N1} \quad \delta q_{0N2}\right]^{T},$$

$$\delta q_{0N1} = \frac{J_{1,2}(q)}{J_{1,1}(q)^2 + J_{1,2}(q)^2}\delta q_{01} + -\frac{J_{1,1}(q)J_{1,2}(q)}{J_{1,1}(q)^2 + J_{1,2}(q)^2}\delta q_{02} = \\ = \frac{l_2 s_{12}}{\left(l_1 s_1 + l_2 s_{12}\right)^2 + \left(l_2 s_{12}\right)^2}\delta q_{01} + \frac{-\left(l_1 s_1 + l_2 s_{12}\right) l_2 s_{12}}{\left(l_1 s_1 + l_2 s_{12}\right)^2 + \left(l_2 s_{12}\right)^2}\delta q_{02}, \tag{32}$$

$$\delta q_{0N2} = -\frac{J_{1,1}(q)J_{1,2}(q)}{J_{1,1}(q)^2 + J_{1,2}(q)^2}\delta q_{01} + \frac{J_{1,1}(q)}{J_{1,1}(q)^2 + J_{1,2}(q)^2}\delta q_{02} = \\ = \frac{-\left(l_1 s_1 + l_2 s_{12}\right) l_2 s_{12}}{\left(l_1 s_1 + l_2 s_{12}\right)^2 + \left(l_2 s_{12}\right)^2}\delta q_{01} - \frac{l_1 s_1 + l_2 s_{12}}{\left(l_1 s_1 + l_2 s_{12}\right)^2 + \left(l_2 s_{12}\right)^2}\delta q_{02}.$$

Visualization of the MRR-R1 configuration space with the particular and nullspace solution of (14) is given in Fig. 7.

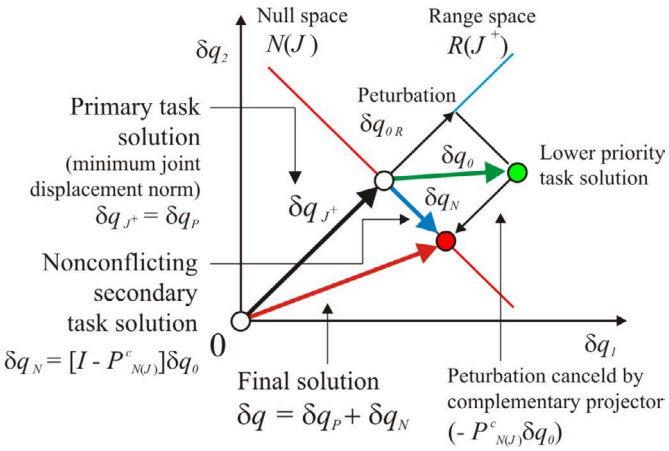

Fig. 7 – *Particular and nullspace solution of MRR-R1 derived from* (18).

Since the dimensionality of the task space is $m = 1$, then the stiffness matrix is a scalar, i.e., $K_x = k_x$. Its transformat in the jointspace is then:

$$K_q = k_x \begin{bmatrix} J_{1,1}^{\ 2}(q) & J_{1,1}(q)J_{1,2}(q) \\ J_{1,1}(q)J_{1,2}(q) & J_{1,2}^{\ 2}(q) \end{bmatrix}, \tag{33}$$

and consequently, in accordance to (19), the cost function is:

$$u(q) = k_x \left\| J_{1,1}(q)J_{1,2}(q) \right\| = k_x l_2 s_{12} \left(l_1 s_1 + l_2 s_{12} \right), \tag{34}$$

which finally leads to the gradient optimization function:

$$\delta q_0 = \begin{bmatrix} -k_x \sin(2q_1 + 2q_2) l_2^{\ 2} - k_x l_1 \sin(2q_1 + q_2) l_2 \\ -k_x l_2 \cos(q_1 + q_2)\left(2 l_2 \sin(q_1 + q_2) + l_1 \sin(q_1)\right) \end{bmatrix}. \tag{35}$$

Generated scalar potential field of the cost function (34) is shown in Fig. 8a, together with corresponding stream lines which are calculated using relation (35). The potential field (35) is well-behaved and the corresponding stream lines converge steadily to the nearest local minima.

The TCP stiffness map over the entire jointspace is shown in Fig. 8b. This stiffness map is derived using equation (17) and the jointspace stiffness matrix (33), which is reduced to its diagonal elements only (off-diagonal elements are simply disregarded because MRR-R1 robot is not able to generate them). Since there exists at least one configuration subspace $Q \subseteq \mathrm{N}(J(q))$ with a nonempty set of configurations $q^* \in Q \wedge Q \neq \varnothing$ which simultaneously satisfies constraints 2 and 3, it is clear that the hypothesis which is defined in a Section 3 holds partially for the MRR-R1 robot.

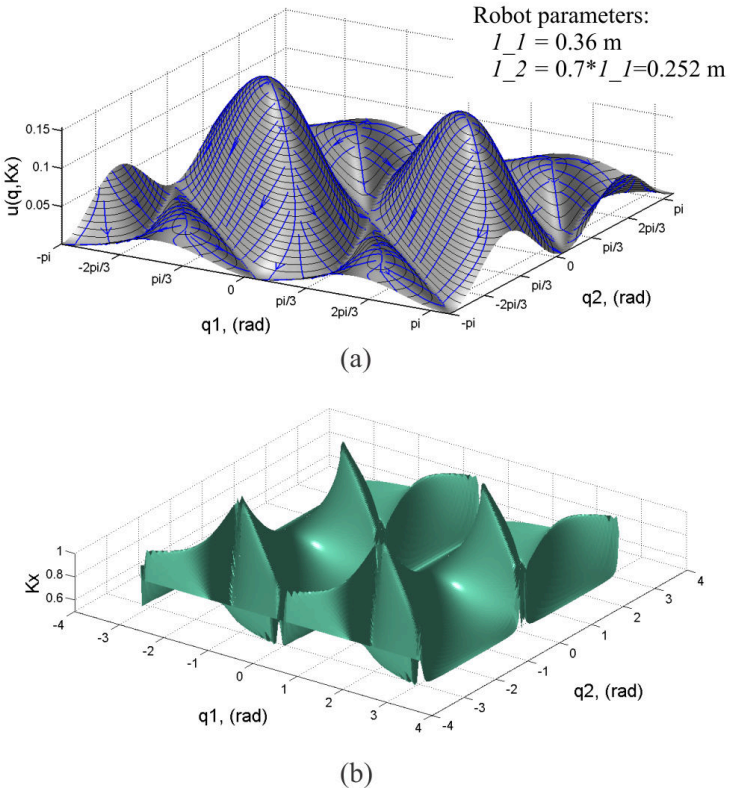

Fig. 8 – (a) *Potential field and the corresponding stream lines generated by equation* (34) *and* (35)*;* (b) *TCP stiffness map of the MRR-R1 over the entire jointspace.*

To prove completeness of the defined hypothesis it is necessary to test the consistency of the $q^* \in Q$ with the constraint 1. For that purpose a series of simulation experiments were performed based on integration scheme (18). In Fig. 9 are shown the simulation results which are related to the case when both, primary and secondary tasks are active and when the value of β multiplier in the α operator (19) is set to 1. The TCP motion of the MRR-R1 robot mechanism shown in Fig. 9, leads to the conclusion that the task inference machine (14) effectively accomplishes both the primary and secondary task, with stable convergence to the secondary task optimum, governed by the cost function (19) and the corresponding nullspace motion generator (20). The convergence of the secondary task to its optimal value is faster than the convergence of the primary task, i.e., the optimal value of the TCP stiffness $k_x = k_{xd}$ is achieved in the integration step $k = 241$, while the TCP desired position x_d is achieved in the integration step $k = 359$, even though the norms of the particular and nullspace displacement are the same (according to (19) and $\beta = 1$).

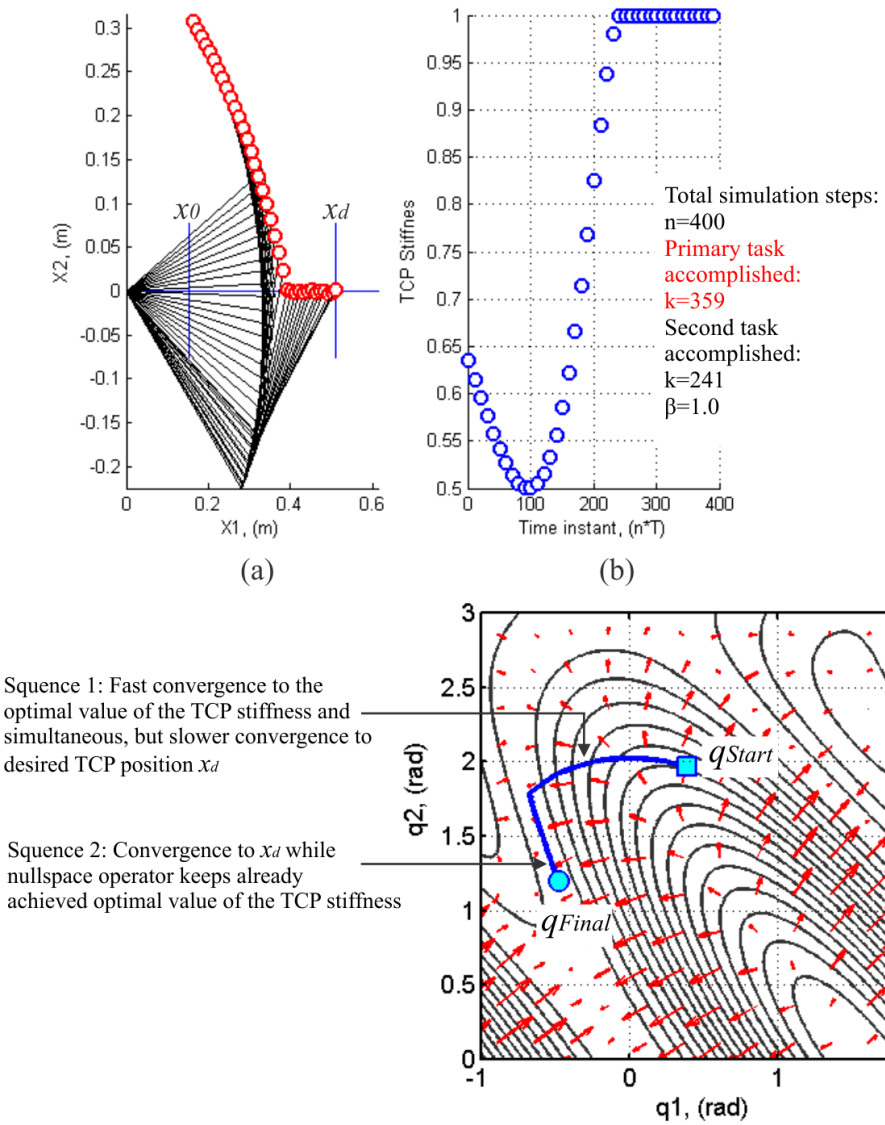

Fig. 9 – *Simulation results of the MRR-R1 robot motion from* x_0 = (l1+l2)/4 = 0.153 m *up to* x_d = (l1+l2)/1.2 = 0.510 m *and execution of the secondary task – optimization of the TCP stiffness:* (a) *Robot mechanism motion in the operational space;* (b) *TCP stiffness variation;* (c) *robot motion in the configuration space (isopotential lines and corresponding gradients of the cost function potential field are shown in the background of the plot).*

It is important to underline that once achieved, the secondary task optimum remains stable, i.e., unaffected by the successive changes of the robot configuration before the primary task is completed (integration step k=359). The results obtained from the performed simulation experiments clearly show that the constraint 1 of the hypothesis stated in the Section 3 can be simultaneously satisfied with constraints 2 and 3 by the proposed method in the kinetostatic domain. This proves the validity of the proposed hypothesis for the MRR-R1 robot.

Detailed analytical study has shown that, from purely mechanical point of view, the robot with $n - m > 1$ redundancy possesses significantly richer nullspace capacity then the robot with $n - m = 1$.

Real-world physical evaluation was performed using Yaskawa SIA10F 7d.o.f. anthropomorphic robot arm, reinforced by the dedicated development system which turns existing robot controller into entirely open control system.

For experimental purposes 7 d.o.f. anthropomorphic robot arm is kinematically reduced to 3 d.o.f. redundant configuration in horizontal plane to avoid influence of gravitational terms (open control system allows to lock the other 4 d.o.f.). Performed experiments refers to the influence of the robot self motion (nullspace motion) to the TCP stiffness parameters. Nullspace stiffness measurement setup is shown on Fig. 10.

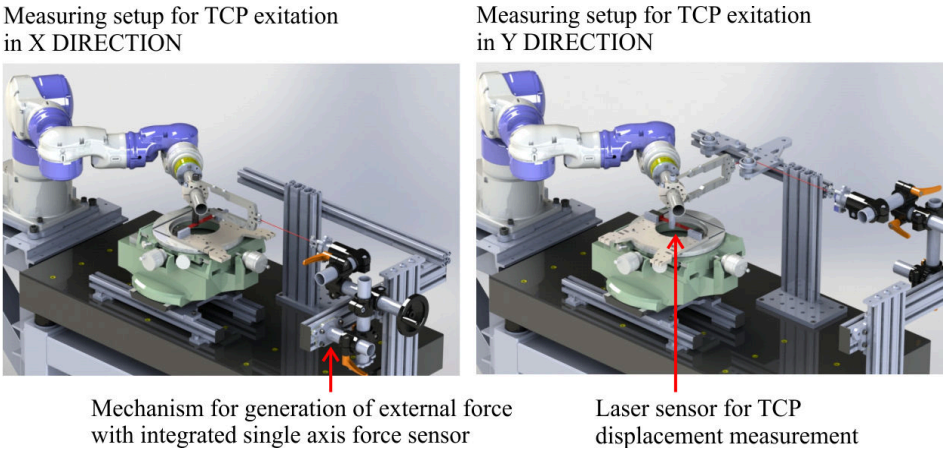

Fig. 10 – *Nullspace stiffness measurement setup.*

Recorded displacements of the TCP in horizontal XY plane for 4 postures in the robot nullspace induced by constant excitation force of 40N applied in X and Y direction is shown on Fig. 11. It is clear the robot nullspace motions have a strong influence to the robot TCP generalized stiffness and also that the robot compliant behaviour is posture dependant and highly nonlinear.

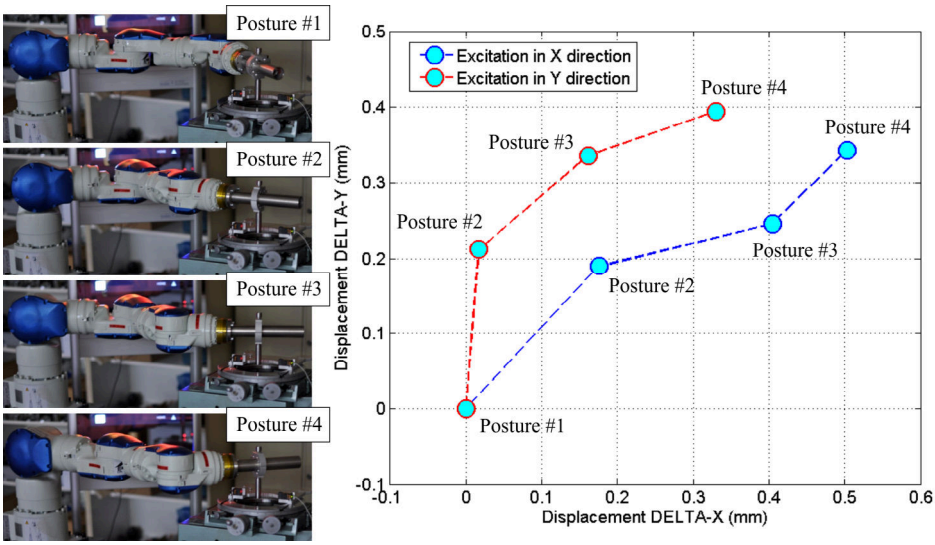

Fig. 11 – *Measured influence of the robot self motion to the TCP stiffness parameters (Robot: Yaskawa SIA10F at CMSys Lab).*

6 Conclusion

Kinematic redundancy and nullspace of the corresponding Jacobian matrix are potentially applicable for effective control of robot TCP compliant behavior by canonization of the jointspace stiffness matrix. High degree of kinematic redundancy, i.e., $r > 1$ is essential to achieve good kinetostatic performances – need to be mathematically analyzed. Euclidean norm of off-diagonal entries of the jointspace stiffness matrix can be effectively used for construction of the cost function for optimization of the robot nullspace stiffness in order to generate best possible approximate of the desired robot TCP stiffness matrix. Problem of computational complexity requires soft-computing (approximate reasoning) and similar techniques to be used. Research in that direction should be included.

7 Acknowledgement

This research is carried out the Cyber-Manufacturing Laboratory - CMSys Lab, Faculty of Mechanical Engineering, within the project: Smart Robotics for Customized Manufacturing, grant No. TR35007, supported by the Serbian Ministry for education, science and technology development.

8 References

[1] A. Liegeois: Automatic Supervisory Control of the Configuration and Behavior of Multibody Mechanisms, IEEE Transactions on Systems, Man and Cybernetics, Vol. 7, No.12, 1977, pp. 868 – 871.

[2] J. Baillieul, J. Hollerbach, R.W. Brockett: Programming and Control of Kinematically Redundant Manipulators, 23-rd IEEE Conference. on Decision and Control, Las Vegas. USA, 12 –14 December 1984, pp. 768 – 774.

[3] O. Khatib: An Unified Approach for Motion and Force Control of Robot Manipulators: The Operational Space Formulation, IEEE Journal of Robotics and Automation, Vol. 3, No. 1, 1987, pp. 42 – 53.

[4] O. Khatib: Motion/Force Redundancy of Manipulators, Japan-U.S.A. Symposium on Flexible Automation, Kyoto, Japan, 1990, pp. 337 – 342.

[5] Ch. Ott: Cartesian Impedance Control of Redundant and Flexible-Joint Robots, Springer Verlag, 2008.

[6] A. Albu-Schäffer, S Haddadin, Ch Ott, A Stemmer, T Wimböck, G Hirzinger: The DLR Lightweight Robot: Design and Control Concepts for Robots in Human Environments, Industrial Robot: An International Journal, Vol. 34, No. 5, 2007, pp. 376 – 385.

[7] J. Salisbury: Active Stiffness Control of a Manipulator in Cartesian Coordinates, 19th IEEE Conference on Decision and Control, 10 – 12 December, 1980, pp. 95 – 100.

[8] N. Hogan: Impedance Control: An Approach to Manipulation, Part I, II and III, ASME Transactions, Journal of Dynamic Systems, Measurement, and Control, Vol. 107, 1985, pp.1– 24.

[9] R. Osu, H. Gomi: Multijoint Muscle Regulation. Mechanisms Examined by Measured Human Arm Stiffness and EMG Signals, Journal of Neurophysiology, Vol. 81, No. 4, 1999, pp.1458 – 1468.

[10] R.V. Patel, F. Shadpey: Control of Redundant Robot Manipulators-Theory and Experiments, Springer Verlag, 2005.

[11] A. Albu-Schaffer, M. Fischer, G. Schreiber, F. Schoeppe, G. Hirzinger: Soft robotics: What Cartesian Stiffness Can We Obtain With Passively Compliant, Uncoupled Joints?, IEEE/RSJ International Conference on Intelligent Robots and Systems, 28 Sept. – 02 Oct. 2004, Vol. 4, pp. 3295 – 3301.

[12] M. M. Svinin, S. Hosoe, M. Uchiyama, Z. W. Luo: On the Stiffness and Stiffness Control of Redundant Manipulators, IEEE International Conference on Robotics and Automation, ICRA′02, Washington DC, 11 – 15 May, 2002, pp. 2393 – 2399.

[13] H. Yanai, K. Takeuchi, Y. Takane: Projection Matrices, Generalized Inverse Matrices, and Singular Value Decomposition, Springer Science and Business Media, New York, 2011.

[14] J. Stuckler, S. Behnke: Compliant Task-Space Control with Back-Drivable Servo Actuators, Proceedings of RoboCup International Symposium 2011: Robot Soccer World Cup XV, LNCS 7416, Springer, 2012, pp. 78 – 89.